

Evolution of ENSO Prediction over the Past 40 Years

Anthony G. Barnston

*International Research Institute for Climate and Society,
The Earth Institute at Columbia University, Lamont Campus, Palisades, NY*

1. What was known by 1975

Since the early to middle 20th century, climate and ocean scientists have come a very long way in their understanding of the El Niño/Southern Oscillation (ENSO) phenomenon, and their ability to predict the ENSO state out to two to four seasons into the future.

Some observational knowledge of ENSO had already been achieved between the 1930s and 1975. Sir Gilbert Walker documented a relationship between the wetness of the Indian monsoon and the sea level pressure and precipitation behavior in various other parts of the world, particularly in the vicinity of the tropical Pacific Ocean (Walker and Bliss 1934). He realized there was a seesaw in sea level pressure between the eastern tropical Pacific region and northern Australia, called the Southern Oscillation, and identified specific weather patterns associated with the two opposing phases of this seesaw. This pressure seesaw also determined the strength of the low-level trade winds and upper level westerly winds that form what we now call the Walker circulation. Later, Berlage (1966) organized and expanded this body of knowledge in an extensive description of the Southern Oscillation and its worldwide teleconnections in the form of seasonally averaged climate anomalies.

A somewhat independent body of knowledge had already existed along the shores of Ecuador and northern Peru, where for several centuries fishermen had noticed that every several years the coastal ocean waters were much warmer than average, particularly around the end of the calendar year. Later in the 1960s, Bjerknes (1966,1969) discovered a physical mechanism for the coupling of the SST anomalies (not only near the South American coast, but well off shore along the equator, toward the international date line) with the sea level pressure anomaly pattern. The key to his discovery is that when the Southern Oscillation is negative (sea level pressure in eastern Pacific below average, and pressure in northern Australia above average), the low-level equatorial Pacific trade winds are weaker than average, and the SST from the central tropical Pacific eastward to the South American coast tends to be warmer than average. Not only did he see this Southern Oscillation – SST relationship, but also hypothesized a positive feedback between the two, so that when one of them deviates from average, the other does likewise, which in turn causes the first to deviate even farther from average, and so forth. This is a key mechanism for the growth of an El Niño (or La Niña) episode. This new understanding of the ENSO phenomena offered explanations for some of its observational aspects, and the long duration of one phase of the seesaw.

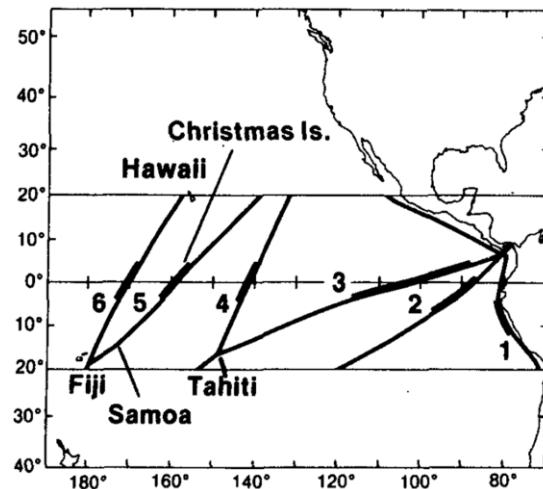


Fig. 1 Ship tracks providing the SST observations used in the analyses of Rasmussen and Carpenter (1982). The heavy portion of each track is the 8° latitude section of maximum interannual SST variability. The time series of monthly average anomalies were computed for this section of each of the 6 tracks.

2. Advances from the mid-1970s to early 1980s

In the mid-1970s, Wyrski (1975) observed changes in sea level associated with ENSO and the zonal wind anomalies in the western tropical Pacific. The latter events, later called westerly wind bursts (because sometimes the total wind direction would actually become westerly instead of the usual easterly), led later to the discovery of equatorial oceanic Kelvin waves and their role in increasing the sub-surface sea temperature during a developing El Niño. Modeling studies in the later 1970s and early 1980 supported these concepts in large-scale ocean dynamics. During that time, however, the subsurface sea temperatures were scantily observed, making a definitive validation difficult.

In the early 1980s Zebiak (1982) applied a model developed from Gill (1980) to the case of ENSO, diagnosing the wind response to an area of heated water in the tropical Pacific. As expected, weakened trade winds resulted from the warmed water, particularly on the west side of the warmed water. Also in early 1980s, Hoskins and Karoly (1981) made major advances in simulating and understanding the global-scale atmospheric responses to El Niño and La Niña. The mechanisms involved heating of the upper atmosphere overlying the warmed water in the tropical Pacific, a strengthening of the Hadley cells both north and south of the equator, and substantial deviations from average of the extratropical circulation patterns (*e.g.*, the jet streams), affecting the seasonal average climate in many regions remote from the tropical Pacific.

A more fully developed observational basis for the theories and models of ENSO described above emerged in a comprehensive study by Rasmussen and Carpenter (1982), showing in detail the wind, SST and rainfall anomaly fields throughout the stages of an El Niño event, based on 6 El Niño events during the 1949-1975 period. During the early 1980s, coverage of SST data in the tropical Pacific was less than what we are used to today in the 2010s. Figure 1 shows the locations of the densest SST data in the early 1980s, coming mainly from ships cruising their standard routes between various ports. The four original “Niño” regions (Niño1, Niño2, Niño3 and Niño4) were defined largely on the basis of the locations of these ship track data sources.

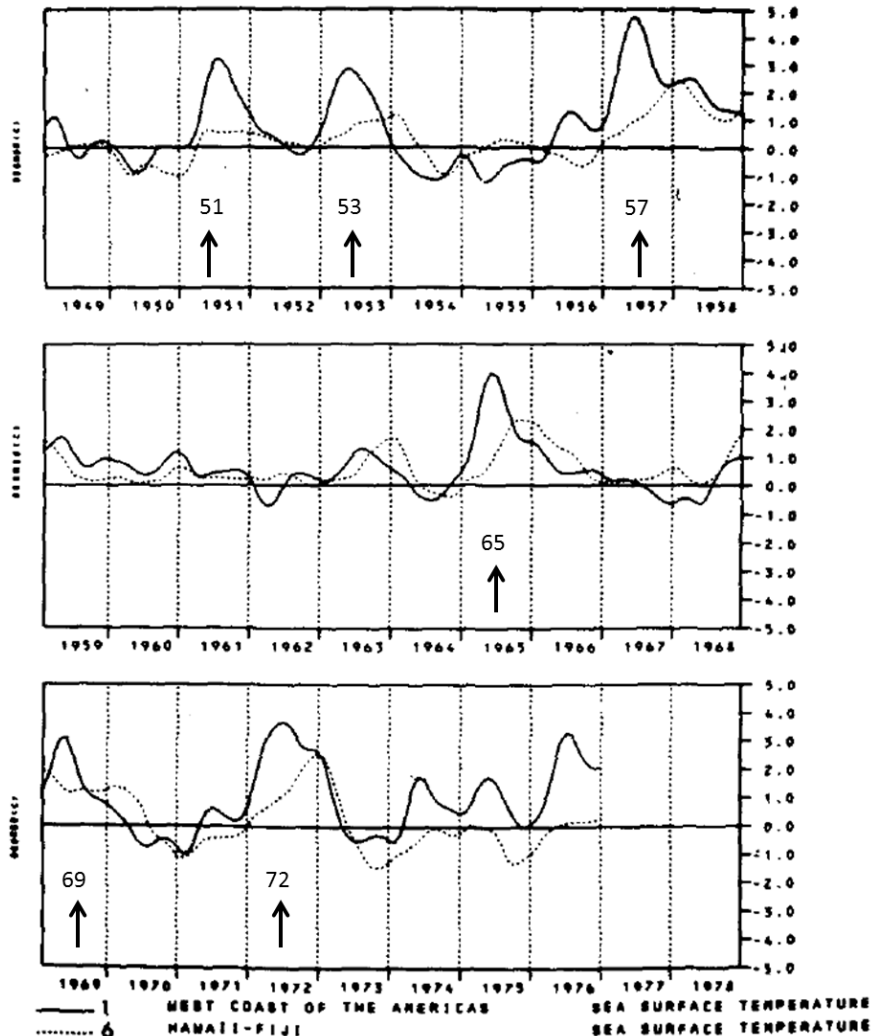


Fig. 2 Time series of SST anomalies in ship track 1 (solid line) and ship track 6 (dotted line) from 1949 to 1978 (see Fig. 1 for ship track numbers). Ship track 1 is closely related to the subsequently defined Niño1+2 region, and ship track 6 to the eastern portion of the Niño4 region (and western boundary of the still later defined Niño3.4 region). The first year of the 6 events used for El Niño composites by Rasmussen and Carpenter (1982) is indicated by a vertical arrow and the year.

Rasmussen and Carpenter (1982) computed composites of various ENSO-related variables based on the 6 El Niño events considered strongest during 1949-1975—namely 1951-52, 1953-54, 1957-58, 1965-66, 1969-70, and 1972-73. At the time of the study, El Niño was regarded largely as a warming along the immediate coast of western South America, with warming farther offshore, out to the dateline, considered a subsequent effect of the primary far eastern Pacific warming. Figure 2 shows time series of SST anomalies in two ship track locations: (1) ship track 1 (along the immediate South American coast) and ship track 6 (crossing the equator near 170°W). The darker line shows the anomaly in ship track 1, consistent with the perception of the coastal SST as the hallmark of El Niño, while the dotted line shows the anomaly at ship track 6. They noted that the eastern Pacific typically warms earliest, followed by a propagation of warming toward the central Pacific several months later. An entire El Niño episode was thought to take place over approximately 1.5 years, going through four phases: (1) onset phase, occurring around December of the year prior to the year of the main event, (2) peak phase, around April of the main year (based on the peak warming in ship track 1), (3) transition phase, around September, and (4) mature phase, occurring in January of the following year. This breakdown of phases is quite different from our current knowledge that events typically begin during April to July, peak during November to January, and die during February to June of the following year. Much of this disagreement is related to the fact that today we consider El Niño as a Pacific basin-wide event, with largest signal in the east-central portion of the basin (Barnston *et al.* 1997), with the far eastern tropical Pacific making up just one small part of the phenomenon (but a part that has great societal impacts along the Ecuadorian and northern Peruvian coasts).

Rasmussen and Carpenter (1982) developed composites of SST and wind anomalies at specified stages of an El Niño event, using the 6 above-mentioned defined events. Figure 3 shows their results for SST anomaly during August-October, low-level wind anomalies during this same season, and SST anomalies during May-July of the year following the main event. These composites, developed using data that were not easily assembled as they could be today, show patterns of SST and wind anomalies roughly consistent with our current knowledge of an El Niño event. Interestingly, the eastern portion of a La Niña pattern is seen in the

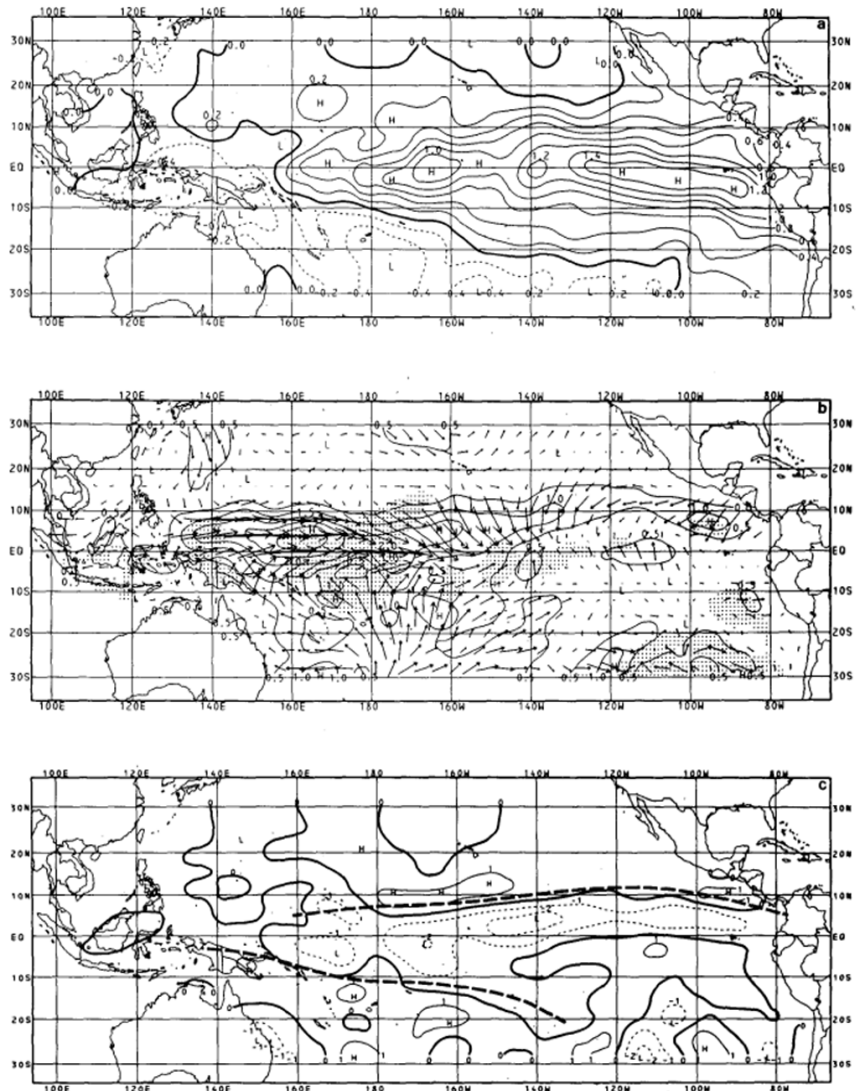


Fig. 3 Composite El Niño anomalies based on 6 events from 1949 to 1976 (see Fig. 2). Top: SST anomaly during August-October of the main year of the event. Middle: Wind anomaly during August-October. Bottom: SST for May-July for the year following the main year of the event. (From Rasmussen and Carpenter 1982.)

composite for early summer of the year following the El Niño, also not inconsistent with what we know today regarding La Niña often following one year after a strong El Niño. Their reliance on just 6 events for the composite, some of which are fairly weak, inevitably engenders sampling issues that would be ameliorated with use of a longer base period.

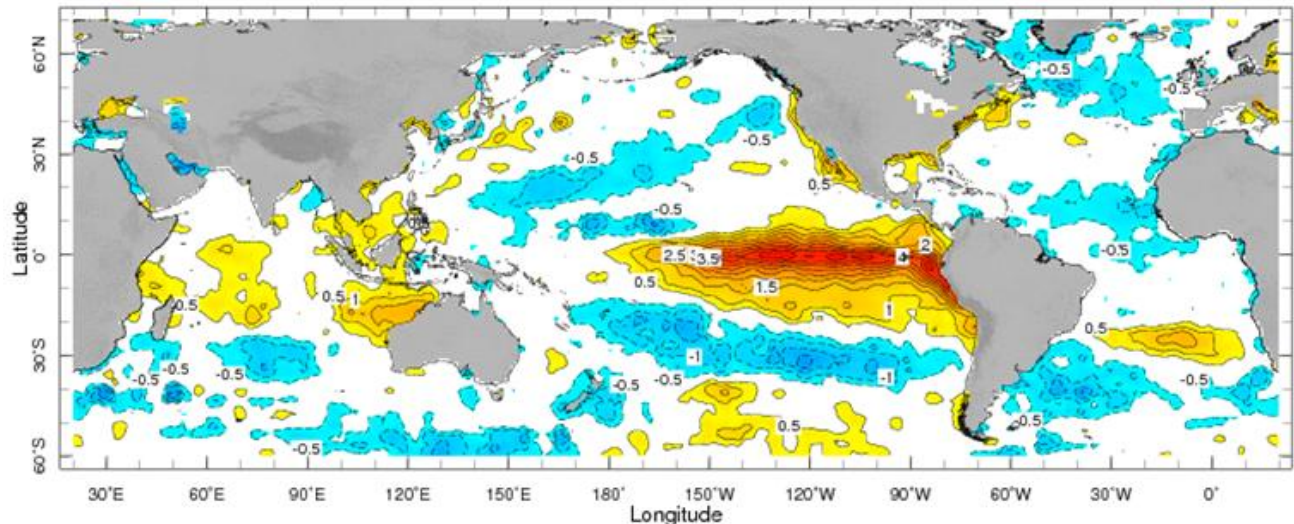


Fig. 4 SST anomaly for December 1982, during the peak of the 1982-83 El Niño, using the merged gauge and satellite data analysis developed long afterwards.

3. The surprise 1982-83 El Niño and the research that followed

The strong 1982-83 El Niño took us nearly completely by surprise. Although it developed steadily in spring and summer 1982, most experts did not recognize it was in progress even at the Climate Diagnostics Workshop in October 1982 when it had become strong. The main reason for this blindness was the lack of coherent, believable data. Satellite data had been developed since the mid-1970s, but there were some breaks in that data before 1979, so a climatology was unable to be defined with so few years in the history. The ship track data were viewed separately from the satellite data, and some of the ship data showed positive anomalies so strong that they were believed to be erroneous, being more than 3 standard deviations above the mean. While this data may have been puzzling, few (or no) leading scientists actually considered that a huge El Niño was in progress. Figure 4 shows the SST anomaly pattern in December 1982, using data that were established long afterwards using the more advanced gauge-plus-satellite merged analysis (Reynolds *et al.* 2002) of today.

The evolution of the 1982-83 El Niño turned out not to follow the stages expected on the basis of the composites of previous El Niño events. The sea level did not build up in the western part of the Pacific basin the year prior to the event as Wyrtki (1975) had observed, and, perhaps more importantly, the warming did not begin in the far eastern part of the basin and propagate westward. Also, new teleconnection regions were noted, expanding the smaller set of regions whose climate was already known to be sensitive to El Niño (*e.g.*, weak Indian summer monsoon, dryness in Indonesia, and differing Pacific island rainfall anomalies).

The surprises related to the 1982-83 El Niño spurred a new wave of ENSO research, most notably the 10-year Tropical Ocean-Global Atmosphere (TOGA) project to study and predict ENSO and its global climate impacts (McPhaden *et al.* 2010). The work coming out of TOGA led to advances in both observational and dynamical fronts. Dynamical models began successfully reproducing ENSO behavior, including the seasonal timing and the 2-7 year periodicity (*e.g.*, Zebiak and Cane 1987; Schopf and Suarez 1988). In Suarez and Schopf (1988), the delayed oscillator theory was put forth. The theory states that besides the eastward-moving oceanic Kelvin waves, westerly wind anomalies also produce westward propagating Rossby waves that reduce subsurface sea temperature, and, after reflecting off the western boundary of the tropical Pacific Ocean (around Indonesia), “kill” El Niño around 6 months after the wind anomaly. In other words, the Bjerknes

positive feedback process is interrupted months later, terminating an El Niño event, as we now know occurs in the first half of the calendar year (often by the end of April) following the year of the main event.

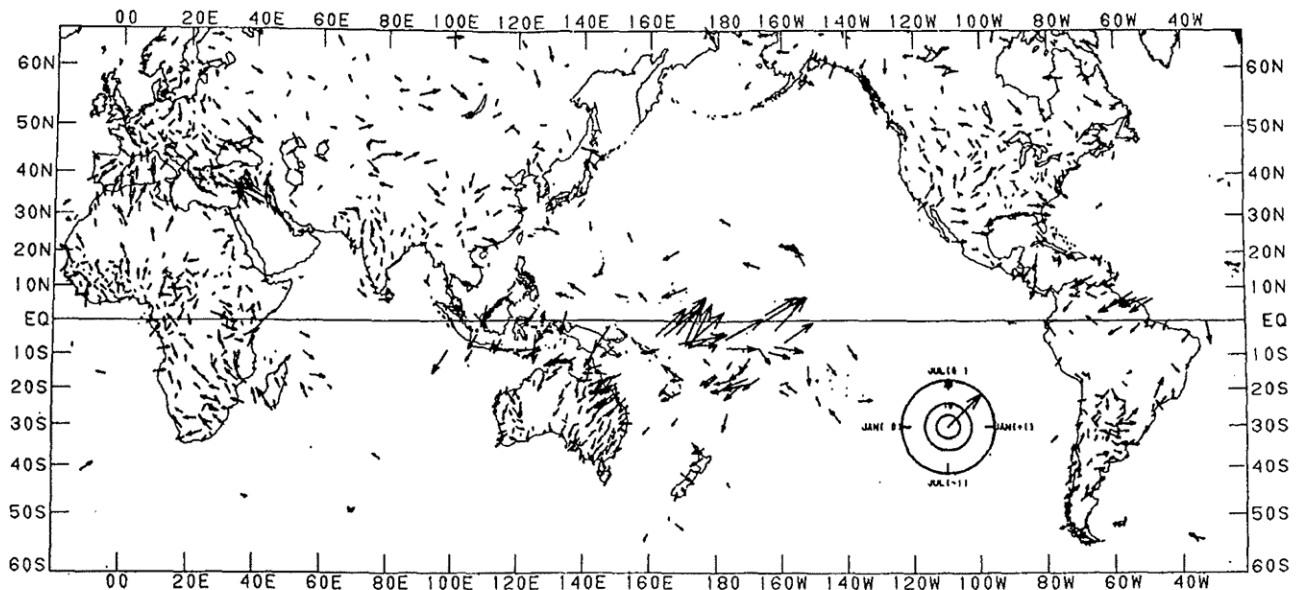


Fig. 5 The strengths and seasons of ENSO composite precipitation, plotted as factors. The vectors are based on a 24-month harmonic fitted to the composites for the ENSO episodes defined on the basis of the Southern Oscillation Index (SOI). The scaling of the vector lengths and directions are defined by the vector clock legend in the figure. Arrows pointing upward indicate above-average rainfall occurring in July of the main El Niño year, and to the right indicate same in January of the year following the main El Niño year. (From Ropelewski and Halpert 1987.)

On the observational side, Ropelewski and Halpert (1987) used a much larger set of data they had organized from the global telecommunication system (GTS), which they called the climate anomaly monitoring system (CAMS; Ropelewski *et al.* 1984), to describe the seasons and locations receiving climate impacts from ENSO. The ENSO state was defined using a long history of the Southern Oscillation Index (SOI) of tropical Pacific sea level pressure, rather than SST whose better data quality began only more recently. Figure 5 shows the ENSO effects on precipitation globally, using vectors showing anomaly strengths and seasonality. Using the vector clock key shown in the figure, we see, for example, that in the southern U.S. there is above-average rainfall during the winter following the main calendar year of the event (arrows pointing toward the right), while in the central tropical Pacific the impact is stronger, and occurs a few months earlier (*i.e.*, around October).

Another very major TOGA-related advance on the observational front was the planning and installation of an extensive system of moored ocean buoys that issued real-time oceanographic and atmospheric data for improved detection, understanding and prediction of El Niño and La Niña (McPhaden *et al.* 1998, 2010). Data from this network (see Fig. 6) is heavily relied upon today, and the particularly important role of the subsurface sea temperature anomalies is widely recognized.

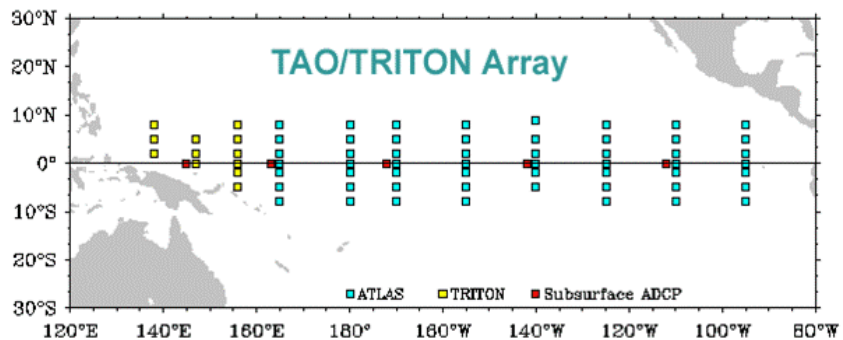


Fig. 6 The configuration of the TAO/TRITON array of moored buoys across the tropical Pacific Ocean, developed in the 1990s in association with the 10-year TOGA program aimed to better understand and predict ENSO. (From the Tao project overview at http://www.pmel.noaa.gov/tao/proj_over/proj_over.html)

4. Systematic development of El Niño/La Niña prediction systems

Improved understanding of ENSO and its location- and season-specific climate effects led to more focused efforts to predict ENSO events and to incorporate their expected climate effects into seasonal climate forecasts. Both empirical and dynamical approaches were used. Empirical (or statistical) methods to predict ENSO, based on antecedent conditions (*e.g.*, tropical Pacific wind or sea level pressure anomalies), were developed by Hasselmann and Barnett (1981), Barnett (1984), and Inoue and O'Brien (1984), among others. These suggested some predictive potential. Successful dynamical simulations of ENSO led to real-time forecasts of ENSO-related SST in the east-central tropical Pacific. The first successful real-time forecast was by Cane *et al.* (1986), where the late forming El Niño of 1986 was predicted by their simple linear dynamical model. By the early 1990s, approaches to ENSO prediction took three paths: (1) purely statistical, as in Barnston and Ropelewski (1992), which used multivariate statistical methods based on latest observed conditions of, *e.g.*, sea level pressure and SST; (2) hybrid statistical/dynamical, as in Barnett *et al.* (1993), where a dynamical ocean model was coupled to a statistical atmospheric model (the wind stress was specified by the ocean model's SST); and (3) dynamical, which progressed from the simple model of Cane *et al.* (1986) to more fully comprehensive, global coupled general circulation models with advanced data assimilation techniques (Latif *et al.* 1993; Ji *et al.* 1994; Stockdale *et al.* 2011).

In the late 1980s and early 1990s, a sizeable portion (but not all) of the potential ENSO predictive skill was already being captured by statistical models and by some hybrid and dynamical models (Barnston *et al.* 1994). Over the course of the 2000s and 2010s, dynamical models gradually became more skillful, while statistical models mainly did not, so that today's best dynamical models slightly outperform statistical models (Tippett *et al.* 2012; Barnston *et al.* 2012). Certain specific weaknesses remain with us when intrinsic predictability is relatively low, such as during the ENSO phase transition period of March-June each year (the so-called ENSO predictability barrier); this weakness is somewhat mollified with the use of subsurface sea temperature anomaly data, as the subsurface anomalies may sometimes act as a bridge to the SST conditions a few months in advance, even during the season of the predictability barrier. ENSO forecasts are usually expressed probabilistically, where a range of outcomes is predicted. The use of a large ensemble of forecasts from a given model, and a combination of such ensemble sets (Kirtman *et al.* 2014), is common practice today. Figure 7 is an example of a multi-model ensemble ENSO forecast from NOAA's Climate Prediction Center in late 2015.

5. Likely improvements in ENSO prediction skill in the future

Even with today's healthy set of state-of-the-art dynamical ENSO prediction models, plenty of examples of large forecast errors still occur. A recent example is the aborted El Niño in late summer 2012, which was forecast to continue to strengthen by most models. Another example is the borderline El Niño of 2014-15,

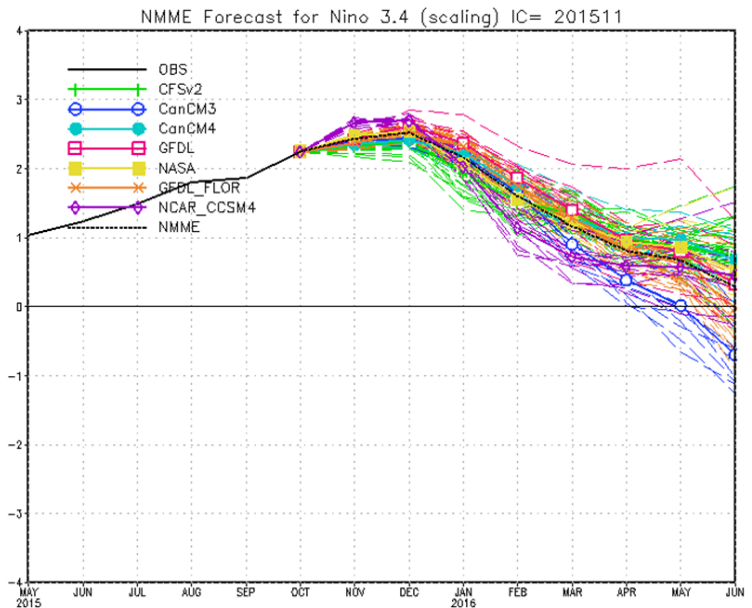


Fig. 7 The North American multi-model ensemble (NMME) forecast for east-central tropical Pacific SST through summer 2016, made from early November 2015 during the peak of the strong El Niño of 2015-16. Individual coupled models are denoted by line colors, and individual ensemble members of each model are visible. The average of the ensemble members of each model is shown by solid colored lines and symbols at each month. The average of all of the ensemble forecasts of all models is shown by the dotted black line.

which was predicted to become a moderate or even strong event by many models in northern spring 2014. Chen and Cane (2008) discussed the extent to which forecasts are limited by intrinsic predictability, versus our suboptimum modeling techniques, and concluded that improvements in our modeling would likely increase ENSO predictive skill noticeably but not greatly. Current modeling weaknesses that can potentially be overcome include an incomplete model representation of all of the relevant physics (*e.g.*, parameterization of processes too small-scale to be captured in data at grid points of the sizes currently used), insufficient observational data (*e.g.*, subsurface sea temperatures), and computer power (for higher spatial resolution, and more ensemble members). Implementing such improvements is currently far too expensive to attempt, but may become increasingly possible in the future. However, even with these weaknesses eliminated, an inherent natural limit of seasonal ENSO predictability is clearly acknowledged, implying that ENSO and climate forecasts will never have average skills as great as those of 1- or 2-day weather forecasts.

Acknowledgements. This study was supported by NOAA's Climate Program Office's Modeling, Analysis, Predictions, and Projections program award NA12OAR4310082.

References

- Barnett, T. P., 1984: Prediction of the El Niño of 1982–83. *Mon. Wea. Rev.*, **112**, 1403–1407.
- Barnett, T. P., M. Latif, N. Graham, M. Flugel, S. Pazan, and W. White, 1993: ENSO and ENSO-related predictability. Part I: Prediction of equatorial Pacific sea surface temperature with a hybrid coupled ocean-atmosphere model. *J. Climate*, **6**, 1545–1566.
- Barnston, A. G., and C. F. Ropelewski, 1992: Prediction of ENSO episodes using canonical correlation analysis. *J. Climate*, **5**, 1315–1345.
- Barnston, A. G., and coauthors, 1994: Long-lead seasonal forecasts—Where do we stand? *Bull. Amer. Meteor. Soc.*, **75**, 2097–2014.
- Barnston, A. G., M. Chelliah, and S. B. Goldenberg, 1997: documentation of a highly ENSO-related SST region in the equatorial Pacific. *Atmos.-Ocean*, **35**, 367–383.
- Barnston, A. G., M. K. Tippett, M. L. L'Heureux, S. Li, and D. G. DeWitt, 2012: Skill of real-time seasonal ENSO model predictions during 2002–11: Is our capability increasing? *Bull. Amer. Meteor. Soc.*, **93**, 631–651.
- Berlage, H.P., 1966: The Southern Oscillation and world weather. *Mededelingen en verhandelingen*, **88**, 152 p.
- Bjerknes, J., 1966: A possible response of the atmospheric Hadley circulation to equatorial anomalies of ocean temperature. *Tellus*, **18**, 820–829.
- Bjerknes, J. 1969: Atmospheric teleconnections from the equatorial Pacific. *J. Phys. Oceanog.*, **97**, 163–172.
- Cane, M. A., S. E. Zebiak, and S. C. Dolan, 1986: experimental forecasts of El Niño. *Nature*, **321**, 827–832.
- Chen, D., and M. A. Cane, 2008: El Niño predictions and predictability. *J. Comput. Phys.*, **227**, 3625–3640.
- Gill, A. E., 1980: Some simple solutions for heat-induced tropical circulation. *Quart. J. Roy. Meteorol. Soc.*, **106**, 447–462.
- Hasselmann, K., and T. P. Barnett, 1981: Technique of linear prediction for systems with periodic statistics. *J. Atmos. Sci.*, **38**, 2275–2283.
- Hoskins, B. J., and D. J. Karoly, 1981: The steady linear response of a spherical atmosphere to thermal and orographic forcing. *J. Atmos. Sci.*, **38**, 1179–1196.
- Inoue, M., and J. J. O'Brien, 1984: A forecast model for the onset of a major El Niño. *Mon. Wea. Rev.*, **112**, 2326–2337.
- Ji, M., A. Kumar, and A. Leetmaa, 1994: An experimental coupled forecast system at the National Meteorological Center: Some early results. *Tellus*, **46A**, 398–418.

-
- Kirtman, B. P., and Coauthors, 2014: The North American Multi-Model Ensemble: Phase-1 seasonal to interannual prediction; phase-2 toward developing intra-seasonal prediction. *Bull. Amer. Meteor. Soc.*, **95**, 585-601.
- Latif, M., A. Sterl, E. Maier-Reimer, and M. M. Junge, 1993: Climate variability in a coupled GCM. Part I: the tropical Pacific. *J. Climate*, **6**, 5-21.
- McPhaden, M. J., A. J. Busalacchi, R. Cheney, J. R. Donguy, K. S. Gage, D. Halpern, M. Ji, P. Julian, G. Meyers, G. T. Mitchum, and others, 1998. The Tropical Ocean-Global Atmosphere (TOGA) observing system: A decade of progress. *J. Geophys. Res.*, **103**, 14,169–14,240.
- McPhaden, M. J., A. J. Busalacchi, and D. L. T. Anderson, 2010: A TOGA Retrospective. *Oceanography*, **23**, 87-103.
- Rasmussen, E. M., and T. H. Carpenter, 1982: Variations in tropical sea surface temperature and surface wind fields associated with the Southern Oscillation/El Niño. *Mon. Wea. Rev.*, **110**, 354-384.
- Reynolds, R. W., N. A. Rayner, T. M. Smith, D. C. Stokes, and W. Wang, 2002: An improved in situ and satellite SST analysis for climate. *J. Climate*, **15**, 1609-1625.
- Ropelewski, C. F. and M. S. Halpert, 1987: Global and regional scale precipitation patterns associated with the El Niño/southern Oscillation. *Mon. Wea. Rev.*, **115**, 1606-1626.
- Ropelewski, C. F., J. E. Janowiak, and M. S. Halpert, 1984: The Climate Anomaly Monitoring System (CAMS). Tech. Report from Climate Analysis Center, NWS, NOAA, Washington DC, 39pp.
- Schopf, P. S., and M. J. Suarez, 1988: Vacillations in a coupled ocean-atmosphere model. *J. Atmos. Sci.*, **45**, 549-566.
- Stockdale, T. N., and coauthors, 2011: ECMWF seasonal forecast system 3 and its prediction of sea surface temperature. *Clim. Dyn.*, **37**, 455-471.
- Suarez, M. J., and P. S. Schopf, 1988: A delayed action oscillator for ENSO. *J. Atmos. Sci.*, **45**, 3283-3287.
- Tippett, M. K., A. G. Barnston, and S. Li, 2012: Performance of recent multimodel ENSO forecasts. *J. Appl. Meteorol. Climatol.*, **51**, 637-654.
- Walker, G., and T. Bliss, 1934: World weather V. *Mem. Roy. Meteor. Soc.*, **4**, 53-84.
- Wyrtki, K., 1975: El Niño—the dynamic response of the equatorial Pacific Ocean to atmospheric forcing. *J. Phys. Oceanogr.*, **5**, 572-584.
- Zebiak, S. E., 1982: A simple atmospheric model of relevance to El Niño. *J. Atmos. Sci.*, **39**, 1179-1196.
- Zebiak, S. E., and M. A. Cane, 1987: A model El Niño-Southern Oscillation. *Mon. Wea. Rev.*, **115**, 2262-2278.